Structural Studies of Novel Siloxysilsesquioxanes

Norbert Auner,*[a] Burkhard Ziemer,[b] Bernhard Herrschaft,[a] Wolfgang Ziche,[c]
Peter John,[c] and Johann Weis[c]

Dedicated to Prof. Dr. Peter Jutzi on the occasion of his 60th birthday

Keywords: Silsesquioxanes / MALDI-TOF / DSC / Structure elucidations / Thermochemistry / Mass spectrometry

Five silsesquioxanes $(RSiO_{3/2})_{2n}$ with R = siloxy and n = 4, 5 have been investigated by X-ray crystallography, MALDI-TOF mass spectrometry, and differential scanning calorimetry (DSC).

Silicon and silicon-containing compounds have found widespread use in modern technology; this field includes purely inorganic materials (e.g. for electronics) as well as organosilicon polymers.[1] Especially interesting are globular oligosilsesquioxanes $(RSiO_{3/2})_{2n}$ (n = 3, 4, 5, ...), also called spherosiloxanes due to their shape,[2] in which the Si−O core is trigonal-prismatic (n = 3), cubic (n = 4), or pentagonal-prismatic (n = 5). These are widely used in fields ranging from optical fibres to cosmetics.[3−5] Generally, silsesquioxanes may be best described as an interface between the purely inorganic silicates and carbosilanes composed of a rigid silicate core and chemically useful peripheral organic functionalities. Thus, silsesquioxanes serve as precursors for novel organosilicon polymers,[6] organolithiated macromolecular materials,[7][8] and porous hybrid inorganic-organic materials.[9] By virtue of the fact that they are both rigid and polyfunctional, they serve as suitable cores for the formation of three-dimensional dendrimers[10] and liquid crystals.[11] Furthermore, they are useful as templates for the preparation of polymeric and ceramic materials by sol-gel techniques.[12] Their derivatization with organometallic functionalities leads to precursors for catalyst preparation (e.g. cobalt carbide nanoparticles in a siliceous matrix[13]) or to materials that are useful in electrochemical devices.[14]

The hydrido species $(HSiO_{3/2})_{2n}$ may be employed for the deposition of SiO_2 films in material technology,[15][16] and is widely used as a starting compound for the synthesis of substituted silsesquioxanes.[12][17] The silsesquioxanes also serve as model compounds for the study and understanding of the properties of zeolites and silicates.[18] While crystal structures have been reported for hydrido siloxanes[19] and organosilsesquioxanes,[20] not much is known about siloxy-functionalized silsesquioxanes (or silyl silicates),[21−25] although the pioneering work of Lentz[26] and Hoebbel[27] dates back to the 1960s.

In this paper, we report the crystal structures of five basic siloxysilsesquioxanes (R = $OSiMe_3$, $OSiMe_2H$, $OSiMe_2Vi$ for n = 4, and R = $OSiMe_3$, $OSiMe_2H$ for n = 5). Discrepancies between the structures obtained and the results of ^{29}Si-MAS-NMR studies are clarified by investigation of the thermal behaviour of the cage compounds by DSC. Their suitability as siloxane mass standards for MALDI-TOF mass spectrometry is tested. The siloxysilsesquioxane $[(M_3Q)DQ]_8$, **6** [R = $OSiMe_2(OSiMe_3)$, n = 4], for which no crystal structure could be obtained, was also included in this part of the study.

Molecular Structures

The common structural feature of the present eight-membered cyclic compounds $Si_8O_{20}R_8$ is a heterocubane anion in which the silicon atoms are placed at the corners of a cube, each one bearing a terminal oxygen atom. Twofold bridging oxygen atoms are positioned at each edge of the cube, leading to the coordination formula $[(SiO_{1/1}O_{3/2})^{1-}]_8 = [Si_8O_{20}]^{8-}$ for the core. Eight silyl groups, specifically $SiMe_3$ in **1** $[M_8Q_8]$, $SiMe_2H$ in **2** $[M^H{}_8Q_8]$, and $SiMe_2Vi$ in **3** $[M^V{}_8Q_8]$, are attached to the terminal oxygen atoms, resulting in electrically neutral molecules. Relative to the $[Si_8O_{20}]^{8-}$ anion in Ekanite, $ThKCaNa[Si_8O_{20}]$[28], the Si−O distances in compounds **1−3** are slightly longer and the bond angles at the bridging oxygen atoms have slightly smaller values. This clearly stems from the coordinative requirements in Ekanite, which are essentially dominated by the geometrical constraints imposed by the cations. In **1−3**, these are replaced by bulky SiR_3 substituents with a comparably high steric demand, hence the molecular units are no longer linked together by electrostatic cation interactions, but only by weak dispersion interactions caused by the relatively non-polar silyl groups.

---

[a] Institut für Anorganische Chemie, Johann Wolfgang Goethe Universität,
Marie-Curie-Strasse 11, D-60439 Frankfurt/M., Germany
Fax: (internat.) + 49(0)69/798-29188
E-mail: auner@chemie.uni-frankfurt.de
[b] Institut für Anorganische und Allgemeine Chemie, Humboldt-Universität zu Berlin,
Hessische Strasse 1−2, D-10115 Berlin, Germany
Fax: (internat.) + 49(0)30/2093-6966
E-mail: burkhard=ziemer@chemie.hu-berlin.de
[c] Wacker Chemie GmbH,
Johannes-Hess-Strasse 24, D-84489 Burghausen, Germany

1434−1948/99/0707−1087 $ 17.50+.50/0

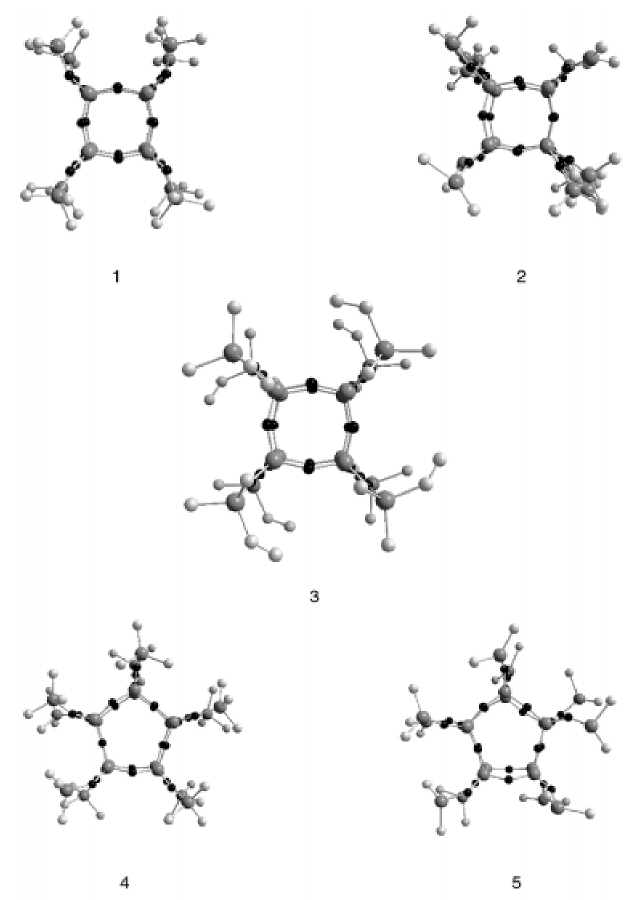

Figure 1. Molecular structures of compounds **1**−**5**

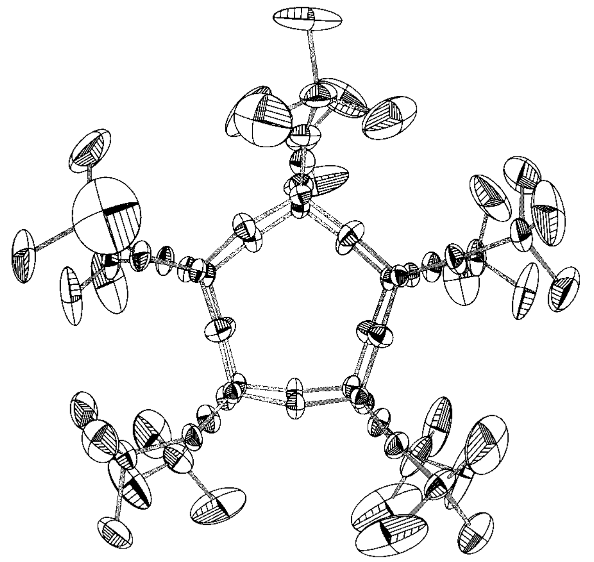

Figure 2. Molecular structure of **4** showing 15% probability atomic displacement ellipsoids

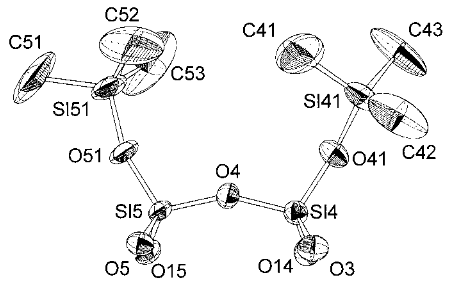

Figure 3. Part of the molecular structure in **5** showing 30% probability atomic displacement ellipsoids

The molecular core of the silsesquioxanes $Si_{10}O_{25}R_{10}$, derived from $[Si_{10}O_{25}]^{10-}$ anions, formally results from the insertion of an $[O(SiO_{1/2}O_{1/1})_2]^{2-} = [Si_2O_5]^{2-}$ unit into a pseudo-cubic $[Si_8O_{20}]^{8-}$ anion, leading to a pentagonal-prismatic anion $[(SiO_{1/1}O_{3/2})^{1-}]_{10} = [Si_{10}O_{25}]^{10-}$. Isolated anions of this type have not been observed in the solid state, but they do occur as building blocks in zeolites (pentasil units in ZSM-5 and ZSM-11)[29]. The novel cyclic silicates $Si_{10}O_{25}R_{10}$ (**4**, R = $SiMe_3$, $M_{10}Q_{10}$; **5**, R = $SiMe_2H$, $M^H{}_{10}Q_{10}$) may be regarded as model compounds of the anions $[Si_{10}O_{25}]^{10-}$ characterized as their silyl-substituted molecular entities. The geometrical features are similar to those discussed for $Si_8O_{20}R_8$. The molecular structures of the silsesquioxanes **1**−**5** have been determined by single-crystal X-ray diffraction and are shown in Figure 1.

Results and Discussion

As can be seen from Table 1, no unusual interatomic distances or bond angles were detected.[30] As expected, the accuracies of the Si−O and Si−C bond-length determinations are higher for the low-temperature structure analysis and decrease considerably on going from the inner to

Table 1. Variations of bond lengths [Å] and bond angles [°] in molecules **1**−**5** [bond parameters of atoms on split sites are omitted; cage (c) and ligand (l) are distinguished]

	1 T = 295 K	**2** 200 K	**3** 200 K	**4** 295 K	**5** 200 K
$Si-O_c$	1.585−1.616(9)	1.599−1.607(5)	1.597−1.608(3)	1.574−1.609(8)	1.585−1.613(6)
$Si-O_{c/l}$	1.581−1.583(9)	1.585−1.627(7)	1.580−1.606(3)	1.549−1.600(9)	1.568−1.594(6)
$O-Si_l$	1.582−1.587(9)	**not reliable for split sites**	1.594−1.606(3)	1.542−1.610(9)	1.526−1.630(7)
$Si-C_l$	1.66−1.86(3)		1.74−1.99(1)	1.70−1.89(4)	1.62−1.86(2)
$O-Si-O_c$	108.1−110.3(5)	108.9−110.1(2)	108.9−110.1(2)	108.3−110.7(5)	108.1−111.0(4)
$Si-O-Si_c$	147.2−150.5(6)	148.1−148.3(3)	148.1−148.3(3)	149.3−157.9(6)	142.2−156.0(4)
$Si-O-Si_l$	147.8−156.1(7)	159.1−159.1(4)	152.6−153.7(2)	144.8−172.4(8)	141.3−172.4(6)
$O-Si-C_l$	105−114(1)	**not reliable for split sites**	106.0−112.1(3)	105−113(1)	108.8−122.5(7)
$C-Si-C_l$	98−126(2)		107.8−114.1(4)	97−110(2)	110.2−123.7(8)

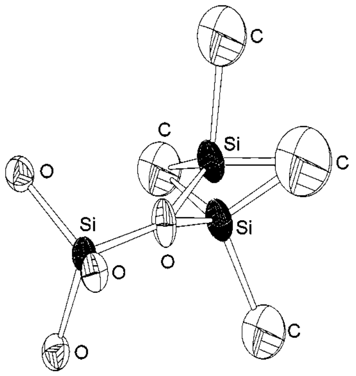

Figure 4. Disorder of $OSiMe_3$ groups in **1** (15% probability, hydrogen atoms omitted for clarity)

the outer sphere within each molecule. This disorder may be explained either in terms of an intense thermal motion of the atoms at room temperature, which is frozen on cooling, or, alternatively, by considering closely neighbouring but slightly different atom positions partially occupied by almost fixed atoms at low temperature.

As mentioned above, these experimental findings may be attributed to a decrease in the rigidity of the core owing to the replacement of metal cations, or in this particular case − following the syntheses of silsesquioxanes **1**−**5** given in the Experimental Section − of ammonium cations $[NR_4]^+$ ($R = CH_3, C_4H_9$), by organosilyl groups. All five structures are characterized by unusually large anisotropic displacement parameters. Figure 2 shows the ellipsoids for **4**, which

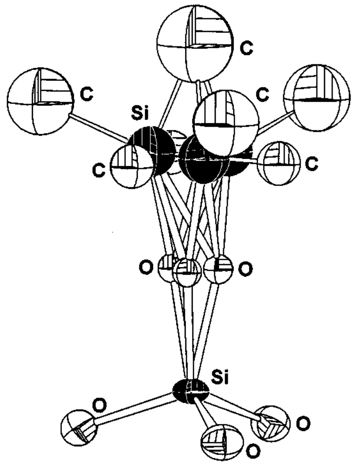

Figure 5. Superposition structure of **2** about the threefold axis; detail of disordered $OSiMe_3$ groups: "ice-cream cone motif"

Table 2. Crystal data, details of data collection and structure refinement for cubes **1**, **2**, **3**, and compounds **4** and **5**

	1	**2**	**3**	**4**	**5**
Empirical formula	$C_{24}H_{72}O_{20}Si_{16}$	$C_{16}H_{56}O_{20}Si_{16}$	$C_{32}H_{72}O_{20}Si_{16}$	$C_{30}H_{90}O_{25}Si_{20}$	$C_{20}H_{70}O_{25}Si_{20}$
M_r	1130.40	1018.16	1226.48	1413.00	1272.7
Crystal system	triclinic	trigonal-rhombohedral	triclinic	monoclinic	monoclinic
Space group	$P{-}1$ (2)	$R{-}3$ (148)	$P{-}1$ (2)	$P21/a$ (14)	$P21/c$ (14)
Crystal size [mm]	0.42, 0.38, 0.22	0.39, 0.23, 0.19	0.62, 0.31, 0.23	1.00, 0.63, 0.12	0.40, 0.38, 0.23
a [Å]	11.046(3)	16.103(3)	11.098(3)	12.636(12)	19.101(4)
b [Å]	11.104(2)	16.103(3)	11.126(3)	44.455(13)	15.029(3)
c [Å]	13.554(2)	17.349(4)	15.006(4)	15.462(4)	22.148(4)
α [°]	77.68(3)		70.15(2)		
β [°]	82.08(4)		71.04(2)	111.90(3)	100.81(2)
γ [°]	84.04(4)		83.59(3)		
V [Å^3]	1603.9(6)	3896(1)	1648.3(8)	8058(8)	6248(2)
$\rho_{calcd.}$ [gcm^{-3}]	1.170	1.302	1.236	1.165	1.354
Z	1	3	1	4	4
$F(000)$ [e]	600	1608	648	3000	2680
μ(Mo-K_α) [mm^{-1}]	0.323	0.395	0.317	0.321	0.41
Data collection					
Diffractometer	STOE Stadi4	STOE Ipds	STOE Ipds	STOE Stadi4	STOE Ipds
Radiation		Mo-K_α, 0.71071 Å graphite monochromator			
T [K]	295(2)	200(2)	200(2)	295(2)	200(2)
Scan mode	$2\theta/\omega = 1.0$	φ oscillat.	φ oscillat.	$2\theta/\omega = 0.5$	φ oscillat.
hkl range	± 10/10/± 13	± 19/± 19/± 21	± 13/± 13/± 18	± 11/42/± 14	± 21/±17/± 25
Measured refl.	4764	11081	16119	12278	39351
Unique refl. (> 2 σ_I)	2982	1714	6010	7480	9731
R_{int}	0.0499	0.0511	0.0508	0.0700	0.0594
Used refl.	2978	1714	6008	7026	9729
Absorption correction	no	no	no	empirical	no
T_{min}/T_{max}	−/−	−/−	−/−	0.8879/0.9995	−/−
Refinement					
Refined parameters	262	93	297	677	586
H atoms (found/calcd.)	0/72	0/56	0/72	0/90	0/70
$R1$[a] [$F_o > 4\ \sigma(F_o)$]	0.1153 (2186 refl.)	0.1008 (761 refl.)	0.0563 (4365 refl.)	0.0809 (4307 refl.)	0.0971 (5393 refl.)
$wR2$[b] (all)	0.2725	0.3032	0.1741	0.3013	0.2747
GooF (all)	1.180	0.961	1.069	1.342	1.070
Weighting par. a, b[c]	0.0830/8.776	0.1884/0.000	0.0902/0.789	0.0650/42.497	0.1040/46.046
ρ_{final}(max/min) [eÅ^{-3}]	0.468/−0.271	0.489/−0.815	0.450/−0.294	0.411/−0.455	2.16/−1.38

[a] $R1 = \Sigma||F_o| - |F_c||/\Sigma|F_o|$. − [b] $wR2 = [\Sigma w(F_o^2 - F_c^2)^2/\Sigma w(F_o^2)^2]^{1/2}$. − [c] $w = 1/[\sigma^2(F_o^2) + (a\ P)^2 + b\ P]$; $P = (F_o^2 + 2\ F_c^2)/3$.

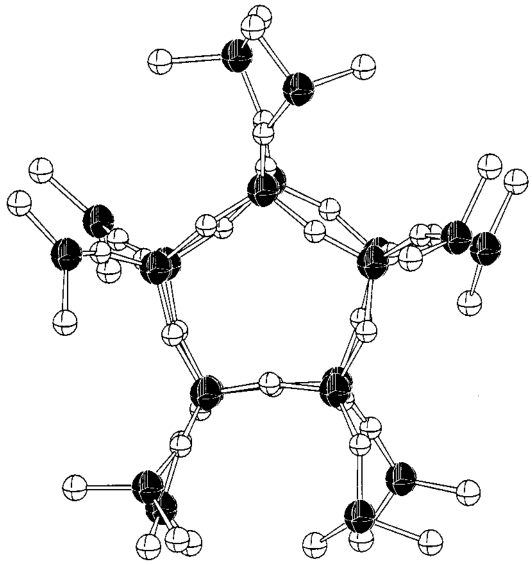

Figure 6. Model structure of **5** with twenty crystallographically independent silicon sites at 200 K

are seen to increase markedly on going from the inner to the outer part of the molecule.

Unusually large anisotropic displacement parameters U_{ij} with $U_3/U_1 > 10$ were found for two peripheral C atoms in **1**, for thirteen C atoms in **4**, and for two C atoms and two ligand Si atoms in **5**. Figure 3 shows a detail of a part of **5** containing one such ligand (Si51, C51, and C52). However, the same figure reveals that the neighbouring ligand (Si41, C41, and C42) does not exhibit unusually large anisotropic displacement parameters.

This indicates atom site disorder, which is individually different for the various ligands and, therefore, cannot be a consequence of a rigid body motion of the whole molecule.

The $OSiMe_3$ groups in **1** are found to be disordered (Figure 4); this may explain why other researchers did not succeed in determining an accurate molecular structure.[21]

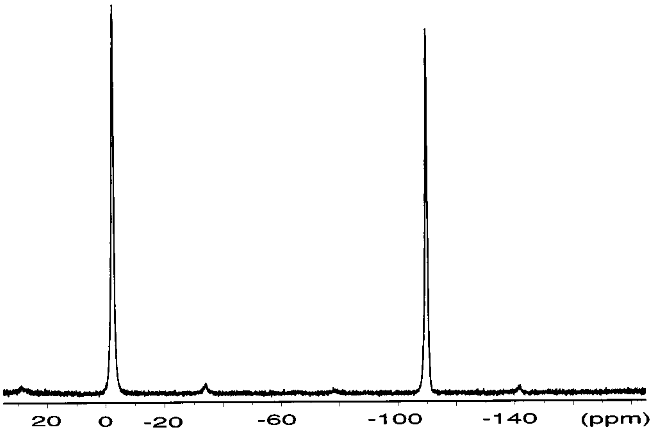

Figure 7. ^{29}Si-MAS-NMR spectrum (spinning rate 2000 Hz) of **5** at 293 K, showing two signals for two sets of ten magnetically equivalent silicon atoms

The highest degree of disorder in all the crystal structures reported in this paper was observed for compound **2**. Here, a split-atom model had to be introduced in order to permit refinement of the atomic positions of all the ligands. Figure 5 shows the superposition structure of **2** about the threefold axis, with each atom site one-third occupied for reasons of symmetry. The ligands at the other corners of the cube are also strongly disordered, but are not subject to any symmetry constraints.

Inspection of the data in Table 2 reveals that **1** and **4** have significantly lower densities than the other silsesquioxanes **2**, **3**, and **5**. In contrast to the other compounds, **1** and **4** have exclusively methyl groups as their outer ligands, which may be a reason for their loose crystal packings.

From the crystal-structure analysis of **5**, it can be seen that at temperatures as low as 200 K (measuring temperature) the whole molecule can be regarded as an asymmetrical unit, with ten crystallographically independent silicon sites making up the core subunit (Figure 6). Notably, in the solid-state ^{29}Si-MAS-NMR spectrum (Figure 7) of the

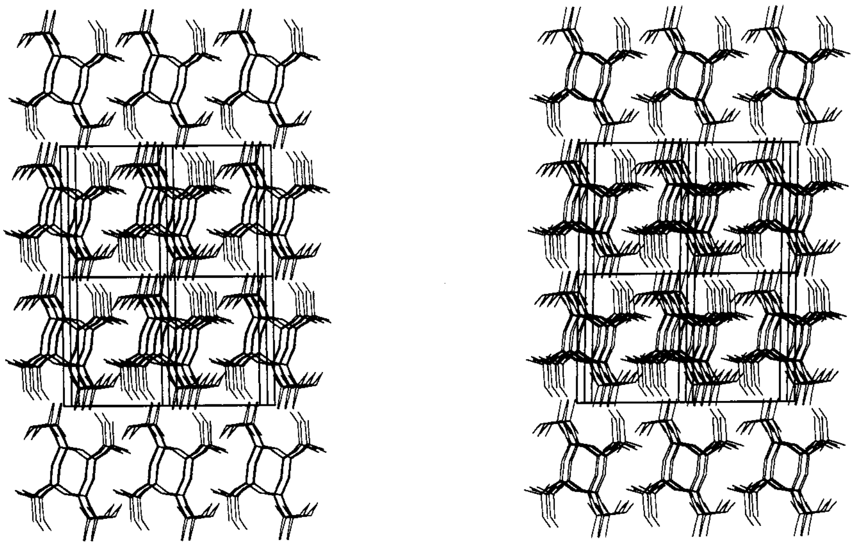

Figure 8. Ordering of **3** in the lattice by interlocking of the vinyl groups; slightly skewed stereo view along the *c* axis

Table 3. Results of DSC measurements

	Measurement details and observations[a]	T [°C]	ΔH [Jg^{-1}] −: endothermic +: exothermic	Interpretation
1	Closed pan, no weight loss	198.8	−6.9	phase transition
		295.4	−2.3	m.p.
		−118.2	endothermic	phase transition
2	Open pan, 49% weight loss	260.3	−15.9	m.p.
	Repetition with same sample, 89% weight loss	>220		m.p. after partial decomposition
	Closed pan, no weight loss	183.9	+4.6	reaction
	TGA, onset of sublimation at 177°C	259.2	−16.7	m.p.
	Closed pan, −140 to +30°C, no weight loss	−117.9	endothermic	phase transition
3	Closed pan, no weight loss	125 (br.)	−4.1	phase transition
		161.8 (br.)	+8.2	reaction
		257.3	−8.7	m.p.
	Repetition with same sample	73.0	−3.3	phase transition
		249.1 and ca. 256	−5.7	m.p.s after partial decomposition
	Open pan, 11% weight loss	125.5	−4.0	phase transition
		253.8	−8.1	m.p.
	Repetition with same sample, 10% weight loss	74.2	−1.3	phase transition
		122.0	−1.9	phase transition
		250.3	−6.4	m.p.
	Closed pan, −140 to +30°C, no weight loss	−45.2	endothermic	phase transition
		−100.0	endothermic	phase transition
4	Closed pan, no weight loss	119.4	−10.0	phase transition
		252.6	−3.2	phase transition
		262.0	−0.7	m.p.
		269.1	+3.3	reaction
	Repetition with same sample	116.8	−9.6	phase transition
		251.4	−3.1	phase transition
		262.0	−1.4	m.p.
		−83.3	endothermic	phase transition
5	Closed pan, no weight loss	83.4	−2.9	phase transition
		135.8	−5.6	m.p.
		143.2	+8.8	reaction
	Repetition with same sample	98.7 (br.)	−3.0	m.p. after partial decomposition
	Open pan, 12% weight loss	83.5	−2.9	phase transition
		135.8	−7.9	m.p.
	Repetition with same sample, 4.7% weight loss	−	−	no phase transition, m.p. or reaction
	Open pan, −100 to +30°C, no weight loss	−60.7	5.0	phase transition
		−44.9	10.6	phase transition
	Closed pan, −140 to +30 °C, no weight loss	24.2	endothermic	phase transition
		−53.3	endothermic	phase transition
		−69.5	endothermic	phase transition
6	Open pan, 100% weight loss at 600°C	144.2	−1.5	phase transition
		232.9	−1.2	phase transition
		> 330−540	−32.9	sublimation
	Open pan, 1.8% weight loss up to 300°C	124.3	−4.0	phase transition
		254.8	−8.1	phase transition
	Closed pan, no weight loss up to 375°C	95.0	endothermic	phase transition
		144.3	endothermic	phase transition
		230.9	endothermic	phase transition
	Closed pan, −140 to +30 °C, no weight loss	18.8	endothermic	phase transition
		−75.5	endothermic	phase transition

[a] Weight loss in open-pan measurements due to sublimation of the compound; measurement up to 300 °C with a 10 °C min^{-1} heating rate.

sample, only two rather than twenty signals appear at ambient temperature, one for the siloxy groups and one upfield-shifted signal for the carbosiloxy groups, indicating the magnetic equivalence of the individual silicon atoms within the two sets of silicon sites.[31]

A better ordering and relative orientation of the silsesquioxanes is achieved by the introduction of vinyl groups into the peripheral silyl substituents at the Si−O core, as exemplified by the crystal structure analysis of **3**. A stereo plot illustrates the interlocking of the vinyl groups (Figure 8).

The findings of (i) the disorder in **1** and **2**, and (ii) the discrepancy between the results of the ^{29}Si-MAS-NMR-spectrometric investigations and of the X-ray analysis of **5** prompted us to measure the DSC curves of the siloxysilsesquioxanes. The results are summarized in Table 3.

Compound **5** shows low-temperature phase transitions (Figure 9). Thus, the differences between the ^{29}Si-MAS-

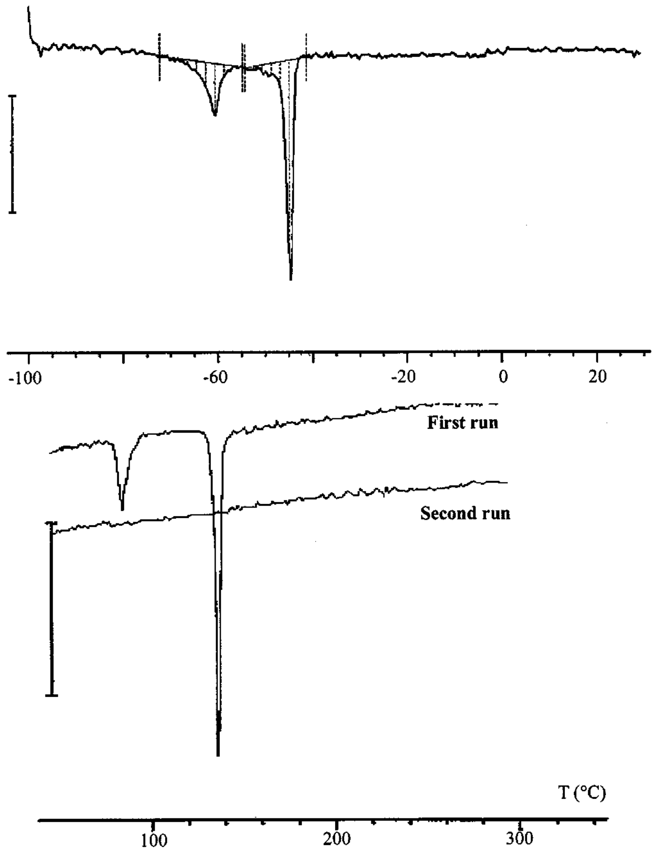

Figure 9. DSC traces of **5** from −100 °C to 30 °C (vertical bar 0.1 Wg^{-1}; 2 °C min^{-1}) and from 30 °C to 300 °C (top trace; 10 °C min^{-1}), repetition with same sample (bottom trace; vertical bar 0.2 Wg^{-1})

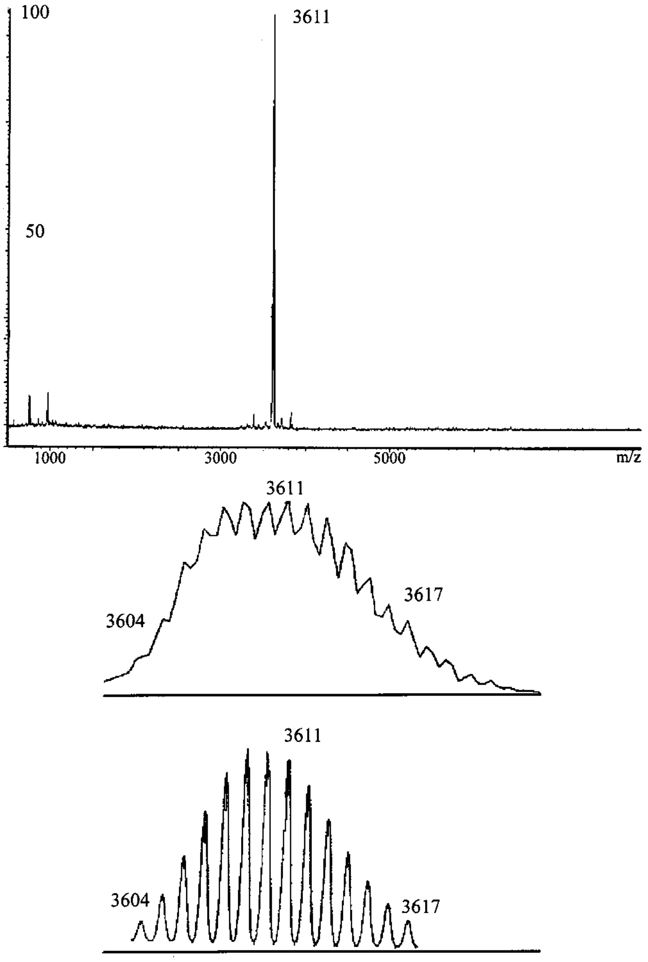

Figure 10. MALDI-TOF mass spectrum of $[(M_3Q)DQ]_8$ (**6**) at *m*/*z* = 3611; insert shows measured and calculated spectrum from *m*/*z* = 3604 to 3620

NMR results and the X-ray crystallography analysis are understandable: While at low temperatures a highly asymmetric modification is stable, at room temperature a much more symmetric arrangement is energetically favoured. Another interesting feature is the low melting point of **5**, which is more than 100 °C lower than those of the other studied silsesquioxanes.

Silsesquioxanes bearing peripheral reactive groups undergo reaction when heated. In particular, **5** reacts completely to form an amorphous glass, which no longer shows any prominent peaks in a subsequent DSC run. ^{29}Si-NMR studies on a sample heated to 220 °C under exclusion of air for 4 h show the formation of $HSiO_{3/2}$ and $Me_2SiO_{2/2}$ groups.

X-ray powder-diffraction experiments were utilized to investigate the nature of two-phase transitions in **1** and **5**.

The diffraction pattern of **1** breaks down at 200 °C. This temperature is in good accord with the phase transition at 199 °C detected by DSC. Simultaneously, **1** begins to decompose and/or to sublime. This behaviour may be explained in terms of the well-known Hedvall effect.[32] The diffraction pattern of **5** changes at 80 °C (upwards) and reversibly at 40 °C (downwards). The high-temperature modification obtained shows a sharp diffraction pattern on the Guinier photograph, but despite this it could not be indexed for a unit-cell determination. A single crystal of **5** heated to 90 °C on a STOE IPDS diffractometer crumbled to a powder, indicating that no topotactic relationship exists between the low- and high-temperature modification.

In addition to structural investigations, compounds **1**−**5** were also characterized by mass-spectrometric methods. Simultaneously, the applicability of the siloxysilsequioxanes as mass standards for **M**atrix-**A**ssisted **L**aser **D**esorption **I**onisation/**T**ime **o**f **F**light (MALDI-TOF) mass spectrometry was investigated (Table 4). Despite the expected high stabilities of the siloxanes, fragmentation and reaction with matrix components was found in some cases. **1** and **2** were found to be contaminated by Q_6M_6[33]; the H-siloxanes reacted with the acidic matrix and showed quite extensive decomposition and fragmentation under the experimental conditions. The excellent result for **3** is not surprising in view of the well-known coordination of carbon−carbon multiple bonds to silver ions. Quite astonishing, however, is the clean spectrum of **6** (Figure 10).[34]

Experimental Section

General: Compounds **1**−**6** were prepared according to known literature procedures[35] by treating freshly precipitated silicic acid

Table 4. Results of MALDI-TOF mass spectrometry

Compound	Fragmentation[a]	Molecular ion[a]
1 Q_8M_8	771 (85%): $Q_6M_6 - Me_3Si$; 1165 (100%): $Q_8M_8 - SiMe_2CH_2$	1237 (77%)
2 $M^H{}_8Q_8$	1253 (100%): $M^H{}_8Q_8$ − H + O-octyl; 3 others below 20%, "noise" ca. 5%	1125 (37%)
3 $M^V{}_8Q_8$		1333 (100%)
4 $Q_{10}M_{10}$	771 (22%) $Q_6M_6 - Me_3Si$; 1743 (100%): ?	1520 (59%)
5 $M^H{}_{10}Q_{10}$	1539 (44%): Si−O−Si in $M^H{}_{10}Q_{10}$ cleaved and substituted by two Me_3Si-O groups; fragments distributed from 1000 to 1700, max. 12%	1379 (100%)
6 $[(M_3Q)DQ]_8$		3611 (100%)

[a] Ag^+ adducts.

with tetramethylammonium hydroxide to form the cyclic octasilicate $[(NMe_4)^+]_8[Si_8O_{20}]$. From the condensation reaction of $Si(OEt)_4$ with tetrabutylammonium hydroxide/H_2O, the decasilicates were obtained. Subsequent treatment of these silicates with mixtures of the corresponding disiloxanes and chlorosilanes or HCl in 2-propanol solution, furnished the octasiloxy- or decasiloxy-substituted silsesquioxanes **1**−**6** in good yields. The representative syntheses of compounds **3** and **5** are depicted in Scheme 1.

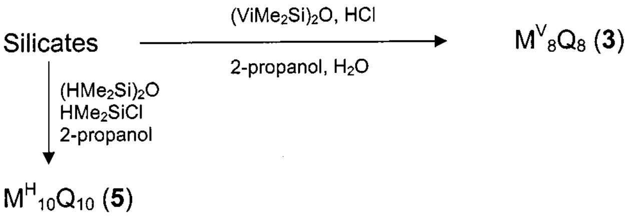

Scheme 1. Syntheses of siloxysilsesquioxanes

The crystalline products thus obtained were recrystallized from CH_2Cl_2/CH_3CN (1:1) by slow evaporation of the solvents at 25°C. Purities were checked by ^1H-, ^{13}C-, and ^{29}Si-NMR spectroscopy in $CDCl_3$ solution.

MALDI-TOF: 10 mg of the sample was dissolved in 1 mL of THF. The matrix solution was made up from 10 mg of 2-nitrophenyl octyl ether in 1 mL of acetone, to which 10 µL of 0.1% trifluoroacetic acid had been added. To assist the ionization, a 0.01 M solution of silver trifluoroacetate in acetone was used. The thin-layer technique was used for sample preparation: 0.5-µL aliquots of the matrix, silver salt, and sample solutions were successively applied. The spectra thus showed the silver adducts. External calibration was carried out with a peptide mixture (substance P and insulin). The mass accuracy was ±1 Da; the masses were rounded to integral numbers.

DSC and TGA measurements were carried out using a Netzsch STA 429 apparatus.

IR and Raman spectra correspond to literature data.[36] Vibrations due to the siloxane framework are assigned as follows (vibrations of organic functional groups are omitted). − IR: 1252−1257 cm^{-1} (s, δ_s $Si-CH_3$), 1074−1098 (vs, ν_{as} Si−O−Si), 755, 844, 868 (s, δ_s Me−Si−O in **1**, **4**, and **6**), 772, 838 (s, δ_s Me−Si−O in **2** and **5**), 621 (m), 559−522 (several s, ν_s Si−O−Si), 901 (s, δ O−Si−H in **2** and **5**). − Raman: Strongest bands at 2902−2912 cm^{-1} (vs, ν CH_3) and 2963−2971 (s, ν CH_3), and at 608−652 (vs, ν_s Si−O−Si); other bands: 1410−1412 (w, δ C−H), 692 (w, ν_s Si−O−Si), several below 420 (w to m, δ O−Si−O); 3057, 1597, 1274, 786 attributable to $-CH=CH_2$ in **3**; 474 (ν_s Si−O−Si) in **6**.

Crystal-Structure Determination: Single crystals of compounds **1** and **4** were examined with a four-circle diffractometer (STOE; STADI4) at room temperature in air. Single crystals of compounds **2**, **3**, and **5** were examined with a one-circle diffractometer equipped with an imaging plate area detector (STOE; IPDS) at 200 K under nitrogen. Intensity data were corrected for Lorentz and polarization effects and in the case of **4** an absorption correction had to be applied (ψ-scan technique[37]) since a crystal of rather anisotropic habit was used for the data collection. The structures were solved by direct methods[38] and refined by full-matrix least-squares techniques against F^2.[39] The thermal motion of all non-hydrogen atoms, better described in terms of atomic displacement parameters (adp's) in the present structures, was treated anisotropically. All hydrogen atoms were calculated in idealized positions and allowed to ride on their corresponding carbon atoms. Their isotropic thermal parameters were set at 1.2 times that of the adjacent C atom. Crystallographic data (excluding structure factors) for the crystal structures reported in this paper have been deposited with the Cambridge Crystallographic Data Centre as supplementary publication no. CCDC-101329. Copies of the data can be obtained free of charge on application to CCDC, 12 Union Road, Cambridge CB2 1EZ, U.K. [Fax: (internat.) + 44-1223/336-033; E-mail: deposit@ccdc.cam.ac.uk]. High-temperature X-ray diffraction on powders of **1** and **5**, representing structure types M_8Q_8 and $M_{10}Q_{10}$, respectively, were carried out with a Nonius Guinier-Lenné camera. The powders were prepared on a platinum gauze and heated to temperatures below their melting points in air or under nitrogen.

---

[1] [1a] *Inorganic Polymers* (Eds.: J. E. Mark, H. R. Allcock, R. West), Prentice Hall, New York, **1992**. − [1b] *Silicon-Based Polymer Science, A Comprehensive Resource* (Eds.: J. M. Zeigler, F. W. G. Fearon), Advances in Chemistry Series 224, American Chemical Society, Washington, **1990**. − [1c] D. A. Loy, K. J. Shea, *Chem. Rev.* **1995**, *95*, 1431. − [1d] *Organosilicon Chemistry II − From Molecules to Materials* (Eds.: N. Auner, J. Weis), VCH, Weinheim, **1996**. − [1e] *Organosilicon Chemistry III − From Molecules to Materials* (Eds.: N. Auner, J. Weis), Wiley-VCH, Weinheim, **1997**.

[2] M. G. Voronkov, V. I. Lavrent'yev, *Top. Curr. Chem.* **1982**, *102*, 199.

[3] G. Calzaferri, *Proc. Tailor-Made Silicon-Oxygen Compounds, Mol. Mater.*, Bielefeld, Sept. 3−5, 1995, **1996**, 149.

[4] H. Bürgy, G. Calzaferri, D. Herren, A. Zhdanov, *Chimia* **1991**, *45*, 3.

[5] R. H. Baney, M. Itoh, A. Sakakibara, T. Suzuki, *Chem. Rev.* **1995**, *95*, 1409.

[6] D. Hoebbel, I. Pitsch, D. Z. Heidemann, *Z. Anorg. Allg. Chem.* **1991**, *592*, 207.

[7] P. A. Agaskar, *J. Am. Chem. Soc.* **1989**, *111*, 6858.

[8] P. A. Agaskar, *Inorg. Chem.* **1990**, *29*, 1603.

[9] P. G. Harrison, R. Kannengiesser, *J. Chem. Soc., Chem. Commun.* **1996**, 415.

[10] A. R. Bassindale, T. E. Gentle, *J. Mater. Chem.* **1993**, *3*, 1319.

[11] F. H. Kreuzer, R. Maurer, P. Spes, *Macromol. Chem., Macromol. Symp.* **1991**, *50*, 215.

[12] V. W. Day, W. G. Klemperer, V. V. Mainz, D. M. Millar, *J. Am. Chem. Soc.* **1985**, *107*, 8262.

[13] P. G. Harrison, R. Kannengiesser, *J. Chem. Soc., Chem. Commun.* **1995**, 2065.

[14] M. Morán, C. M. Casado, L. Cuadrado, J. Losada, *Organometallics* **1993**, *12*, 4327.

[15] S. B. Desu, C. H. Peng, T. Shi, P. A. Agaskar, *J. Electrochem. Soc.* **1992**, *139*, 2682.

[16] M. D. Nyman, S. B. Desu, C. H. Peng, *Chem. Mater.* **1993**, *5*, 1636.

[17] [17a] H. Bürgy, G. Calzaferri, *Helv. Chim. Acta* **1990**, *73*, 698. – [17b] D. Herren, H. Bürgy, G. Calzaferri, *Helv. Chim. Acta* **1991**, *74*, 24. – [17c] G. Calzaferri, D. Herren, R. Imhof, *Helv. Chim. Acta* **1991**, *74*, 1278. – [17d] G. Calzaferri, R. Imhof, *J. Chem. Soc., Dalton Trans.* **1992**, 3391. – [17e] G. Calzaferri, I. Imhof, K. W. Törnroos, *J. Chem. Soc., Dalton Trans.* **1993**, 3741. – [17f] C. Marcolli, R. Imhof, G. Calzaferri, *Microchim. Acta* **1997**, Suppl. 14. – [17g] B. J. Hendan, H. C. Marsmann, *J. Organomet. Chem.* **1995**, *483*, 33. – [17h] U. Dittmar, B. J. Hendan, U. Flörke, H. C. Marsmann, *J. Organomet. Chem.* **1995**, *489*, 185.

[18] [18a] G. Calzaferri, R. Hoffmann, *J. Chem. Soc., Dalton Trans.* **1991**, 917. – [18b] M. Bärtsch, P. Bornhauser, G. Calzaferri, R. Imhof, *J. Phys. Chem.* **1994**, *98*, 2817. – [18c] J. A. W. Harkless, D. K. Stillinger, F. H. Stillinger, *J. Phys. Chem.* **1996**, *100*, 1098. – [18d] V. A. Ermoshin, K. S. Smirnov, D. Bougeard, *Chem. Phys.* **1996**, *202*, 53. – [18e] A. J. M. de Man, J. Sauer, *J. Phys. Chem.* **1996**, *100*, 5025. – [18f] A. M. Bieniok, H.-B. Bürgi, *J. Phys. Chem.* **1994**, *98*, 10735. – [18g] F. J. Feher, D. A. Newman, J. F. Walzer, *J. Am. Chem. Soc.* **1989**, *111*, 1741.

[19] (HSiO$_{3/2}$)$_8$: [19a] T. P. E. Auf der Heyde, H.-B. Bürgi, H. Bürgy, K. W. Törnroos, *Chimia* **1991**, *45*, 38. – [19b] K. W. Törnroos, *Acta Crystallogr.* **1994**, *C5O*, 1646. – [19c] (HSiO$_{3/2}$)$_{10}$: H.-B. Bürgi, K. W. Törnroos, G. Calzaferri, H. Bürgy, *Inorg. Chem.* **1993**, *32*, 4914. – [19d] (HSiO$_{3/2}$)$_{12}$: K. W. Törnroos, H.-B. Bürgi, G. Calzaferri, H. Bürgy, *Acta Crystallogr.* **1995**, *B5l*, 155. – (HSiO$_{3/2}$)$_{14}$: See ref.[16]

[20] See, for example: [20a] R = Me, n = 10: I. A. Baidina, N. V. Podberezskaya, S. V. Borisov, V. I. Alexeev, T. N. Matynova, A. N. Kanev, *Zh. Strukt. Khim.* **1980**, *21*, 125; *Chem. Abstr.* **1980**, *93*, 177686z. – [20b] R = (2-dimethylamino)phenyl, n = 8: R. Tacke, A. Lopez-Mras, W. S. Sheldrick, A. Sebald, *Z. Anorg. Allg. Chem.* **1993**, *619*, 347.

[21] For R = OSiMe$_3$ no entries are found in the Cambridge Crystallographic Database. Two papers, however, report X-ray structures[22]; an ORTEP representation is found in ref.[23], but no further crystallographic details. For R = OSiMe$_3$ and n = 3 a structure is reported in ref.[24] For R = OSiMe$_3$ and n = 5 the cell constants and space group have been determined.[25] For R = OSiMe$_2$H, n = 4, an X-ray structure analysis was reported during the reviewing process of the present paper.[40]

[22] [22a] Y. I. Smolin, F. Shepeler, R. Pomes, *Khim. Silik. Oksidov* **1982**, 68; *Chem. Abstr.* **1982**, *97*, 118501r. – [22b] R. P. Hernández, Y. I. Smolin, Y. F. Shepelev, *Rev. Cient. Univ. Oriente, Cienc. Nat. Mat.* **1977**, *1*, 17.

[23] R. Sasamori, Y. Okaue, T. Isobe, Y. Matsuda, *Science* **1994**, *265*, 1691.

[24] D. Hoebbel, G. Engelhardt, A. Samoson, K. Újszászy, Y. I. Smolin, *Z. Anorg. Allg. Chem.* **1987**, *552*, 236.

[25] D. Hoebbel, W. Wieker, P. Franke, A. Otto, *Z. Anorg. Allg. Chem.* **1975**, *488*, 35.

[26] C. W. Lentz, *Inorg. Chem.* **1964**, *3*, 574.

[27] D. Hoebbel, W. Wieker, *Z. Anorg. Allg. Chem.* **1971**, *38*, 43.

[28] U. I. Moke'eva, N. I. Golovastikov, *Dokl. Akad. Nauk SSSR* **1966**, *167*, 1131; *Chem. Abstr.* **1966**, *65*, 6429d.

[29] C. N. R. Rao, J. Gopalakrishnan, *New Directions in Solid-State Chemistry*, Cambridge Solid-State Science Series, Cambridge University Press, Cambridge, New York, Melbourne, **1986**, p. 40, and literature cited therein.

[30] *International Tables for Crystallography* **1995**, vol. C, Table 9.5.1.1.

[31] M. Backer, A.-R. Grimmer, N. Auner, P. John, J. Weis, *Solid State Nucl. Magn. Reson.* **1997**, *9*, 241. Low-temperature MAS-NMR studies are currently being carried out.

[32] J. A. Hedvall, L. Leffler, *Z. Anorg. Allg. Chem.* **1937**, *234*, 235; and in: K. Hauffe, *Reaktionen in und an festen Stoffen*, Springer-Verlag, Berlin, Göttingen, Heidelberg, **1955**.

[33] Obviously, MALDI-TOF is quite sensitive to Q$_6$M$_6$ contamination as the compound was not found in ^{29}Si- and ^{1}H-NMR spectra.

[34] Unfortunalety, no single crystals could be obtained for **6**, a waxy solid. MALDI-TOF-MS and ^{29}Si-MAS-NMR, however, proved to be valuable analytical tools for the structural analysis of this compound.

[35] [35a] C. Freyer, J. Wolferseder, U. Peetz (Wacker Chemie GmbH), EP 0 624 591 A1, **1994**. – [35b] R. Weidner, N. Zeller, B. Deubzer, V. Frey (Wacker Chemie GmbH), EP 0 367 222 B1, **1989**; *Chem. Abstr.* **1990**, *113*, 11645m. – [35c] R. Weidner, N. Zeller, B. Deubzer, V. Frey (Wacker Chemie GmbH), DE 3837397 A1, **1988**; *Chem. Abstr.* **1990**, *113*, 116465m.

[36] C. Marcolli, P. Lainé, R. Bühler, G. Calzaferri, J. Tomkinson, *J. Phys. Chem.* **1997**, *101*, 1171.

[37] A. C. T. North, D. C. Phillips, F. S. Mathews, *Acta Crystallogr.* **1968**, *A24*, 351–359.

[38] G. M. Sheldrick, *Acta Crystallogr.* **1990**, *A46*, 467.

[39] G. M. Sheldrick, *Program for Crystal Structure Refinement*, Universität Göttingen, Germany, **1993**.

[40] A. Provatas, M. Luft, J. C. Mu, A. H. White, J. G. Matisons, B. W. Skelton, *J. Organomet. Chem.* **1998**, *565*, 159.

[I98330]